Journal of Renewable Materials

Tech Science Press

Mechanical Properties of a Eucalyptus-Based Oriented Oblique Strand Lumber for Structural Applications

Jiawei Chen[1], Haibei Xiong[1,*], Zhifang Wang[1] and Linqing Yang[2]

[1]College of Civil Engineering, Tongji University, Shanghai, 200092, China.

[2]Shenzhen Plantation Material Technology Co., Ltd., Shenzhen, 518055, China.

[*]Corresponding Author: Haibei Xiong. Email: xionghaibei@tongji.edu.cn.

Abstract: Wood and wood-based composite materials have gained increasing attention in the sustainable building industry because of their renewability and environmental friendliness. Oriented oblique strand lumber (Eucalyptus Strand Wood, ESWood), which is manufactured from fast-growing small diameter eucalyptus wood (*Eucalyptus urophylla* × *E. grandis*), is introduced in this paper. Small clear specimen tests were conducted to determine the mechanical properties of ESWood material while full-scale component tests were performed to observe the structural performance of ESWood beams. A comparison of mechanical properties of ESWood with other wood/bamboo-based materials is then reported. From the results presented herein, it appears that the strength and stiffness properties of ESWood are affected by grain directionality and glued layers. However, it still has preferable mechanical properties as a building material, which is comparable or superior to those of other engineered wood/bamboo-based products (e.g., Sitka spruce, LVL, OSL, Glulam, and Glubam). Furthermore, results from full-scale component tests show the stable mechanical performance of beams made by ESWood. This study makes a significant contribution to a potential utilization of fast-growing eucalyptus for general use in construction, and the presented mechanical tests results can serve as a fundamental data for more applications of ESWood in practical engineering.

Keywords: Wood-based composite material; mechanical properties; eucalyptus; experimental test; construction material

1 Introduction

With the increasing need for renewable and sustainable construction materials in the building industry, wood, because of its carbon storage, renewability and environmentally friendly characteristics, has gained more attention nowadays. However, due to the dramatic decreasing number of natural forests and stricter environmental protection laws, fast-growing wood including eucalyptus is expected to be used in building structures because of its ease of reproduction [1].

As one of the three fast-growing species in the world, the global yield of eucalyptus is quite considerable. Nowadays, eucalyptus is planted in more than 90 countries around the world, with over 20 million hectares of plantations [2]. Meanwhile, with the genetic improvement and industrialization technologies development, there are a few attempts to employ eucalyptus as solid sawn lumber to build log houses in Brazil in recent years [3]. However, currently most eucalyptus is still used to produce pulp and paper, and are rarely used in structural applications because it is considered to be non-durable and uneconomic, with high dimensional instability and treatment difficulty [4].

As the increasing demand for wood-based structural materials, considerable efforts have been made to develop engineered eucalyptus-based composite materials, which combine the best properties of eucalyptus with other materials (e.g., adhesives, plastics, etc.) to produce new products that satisfy structural demands. Similarly with other engineered wood/bamboo-based composites [5,6], the eucalyptus

wood is peeled, chipped, or sliced to small pieces and then reconstituted to form large members during the manufacturing process. In this way, natural macro defects in eucalyptus are dispersed, and the material strength and stability are significantly increased compared with the solid eucalyptus sawn lumber, which suggests the potential of eucalyptus-based composite materials to be used as structural elements in building constructions.

Many engineered eucalyptus-based products have been proposed in recent years. Initially, eucalyptus-based particleboard was developed since it does not need high-quality raw materials [7]. According to previous researches, special treatments (e.g., steaming process, hot water treatment), resin content and press time are the main factors affecting the properties of particleboards made from eucalyptus [8-10]. Currently, laminated veneer lumber (LVL), which is manufactured by laminating veneer with all piles parallel to the length, has been developed as an important wood product for building construction because of its advantages of uniform engineering properties and dimensional flexibility. An increasing amount of studies on the physical and mechanical properties of LVL panels produced from eucalyptus emerged in recent years. It was found that eucalyptus-based LVLs are comparable to those made from poplar, Beech, and even Norway spruce [11-16]. However, it was also summarized that various problems still exist in the production of eucalyptus-based LVLs, including the glue difficulty, end-splits, and breakage of sheets of veneer [11].

Investigation on performance of structural size eucalyptus-based glued laminated timber (Glulam) was also conducted, mainly focusing on the influence of geometric and material parameters, adhesive types, and failure modes on mechanical performance [17-20]. With high levels of characteristic strength and modulus of elasticity, the Glulam made from eucalyptus is considered to be used as structural elements in building constructions. Meanwhile, recently, several attempts were made to use fast-grown small diameter eucalyptus for manufacturing cross-laminated timber (CLT), and researchers found that eucalyptus CLT made of small diameter lumber was comparable to commercial softwood CLT for structural applications [21,22].

Oriented strand lumber (OSL), similar to LVL, is the newest product of the structural composite lumber (SCL) family. It is manufactured using strands of wood or strips of veneer with a primary orientation along the length of the member. Several studies have been conducted to determine the mechanical properties of OSL made from rubberwood [23], parawood [24], poplar [25], and bamboo [26]. However, few studies have investigated the mechanical properties of eucalyptus-based OSL.

In this paper, an innovative oriented oblique strand lumber manufactured from fast-grown small diameter eucalyptus wood is introduced, which is a patented product with a trademark of ESWood (Eucalyptus Strand Wood, ESWood). ESWood is made by strands of eucalyptus veneer, which are oriented in parallel along the length of the member, with a certain oblique angle (usually 45°) between the width direction of the strands and the thickness direction of the members. An aesthetic appearance with wood texture on four sides of the components is obtained by this manufacturing technique, which is quite different from the existing OSL products. This paper introduces the production of ESWood, investigates its main mechanical properties by small clear specimen tests, and also provides a comparison between ESWood and other wood/bamboo-based materials.

2 Production of ESWood

Production processes of ESWood can be divided into four steps, including raw eucalyptus selection, making veneer strands, gluing and pressing, and post-processing. It should be noted that the production processes solve the difficulties of drying, sawing, and gluing eucalyptus wood, which enhances the mechanical performance of the eucalyptus material.

2.1 Raw Eucalyptus Selection

Firstly, the eucalyptus wood which meets the requirement for maturity is selected and prepared for making the veneer. Fast-growing eucalyptus wood (*Eucalyptus urophylla* × *E. grandis*) aged 6-8 years

from eucalyptus plantation is used as the raw material of ESWood. Generally, the average diameter of eucalyptus trunks of this age can reach 10 cm or larger. Fig. 1(a) demonstrates a batch recently harvested eucalyptus logs at a plantation in Guangdong, China. The eucalyptus logs are then transported to the production factory for the subsequent processes.

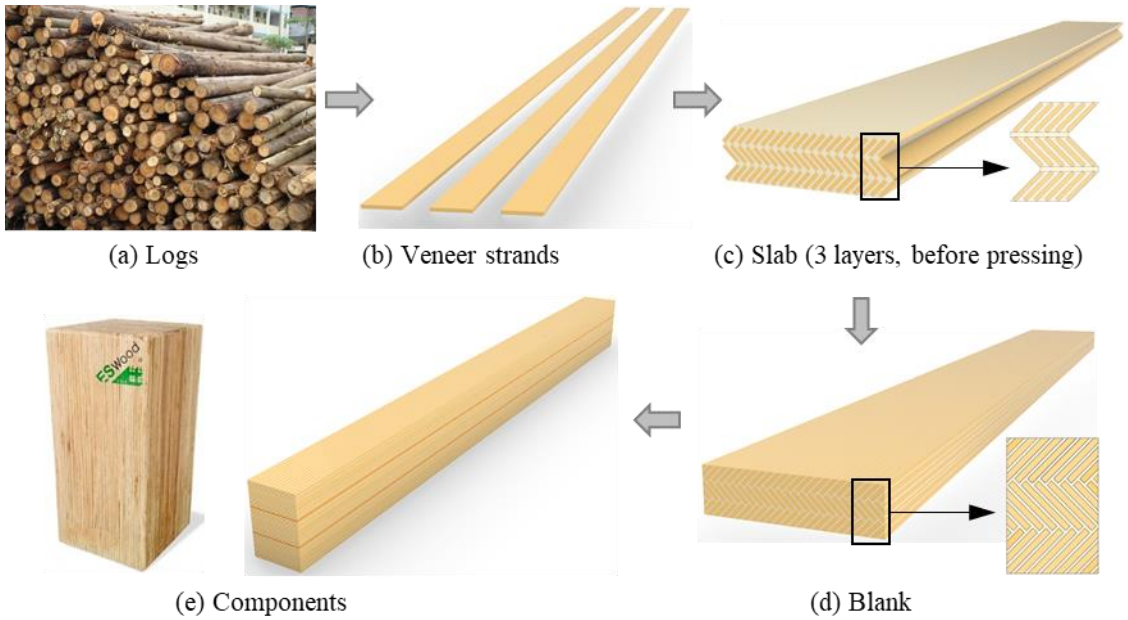

Figure 1: Production of ESWood: (a) Raw eucalyptus logs; (b) Eucalyptus veneer strands; (c) Slab formed by resin saturated strand layers; (d) Blank; (e) ESWood components

2.2 Eucalyptus Veneer Strands

The eucalyptus logs in the factory are firstly peeled circumferentially to form veneers, which are then dried to around 12% moisture content (MC) for the preparation for veneer strands making. The quality of eucalyptus veneer strands is fundamental to the physical and mechanical properties of ESWood. Compared with the processing techniques of LVL [27,28] and parallel strand lumber (PSL) [29,30], the eucalyptus veneers are cut into thicker and more slender strands due to the factors of the diameter of eucalyptus logs, the shape and the dimension of the components, etc., which are in the range of 2-4 mm thickness, 5-30 mm width, and 400-1300 mm length, as shown in Fig. 1(b). Meanwhile, in order to make the slab density uniform, strands with the same thickness (usually 3 mm) are used to produce the same slab.

2.3 Gluing and Pressing

The eucalyptus veneer strands are then saturated in phenol formaldehyde resin which concentration is 30~45%. The resin was a commercial product manufactured by a company in Guangdong Province. Its basic parameters include solid content of 43.5%, pH value of 7.54 and viscosity of 80 (cps 30°C). The resin-saturated strands are dried to around 8% moisture content.

Depending on the pre-designed proposal for the single layer and the components, dozens of layers of resin-saturated strands are stacked in parallel along length direction in the mold, with a certain angle (usually 45°) between the width direction of the strands and the thickness direction, as shown in Fig. 1(c). After that, usually three layers with adhesive in between in the mold are moved to the cold press machine for reassembly and cold-press forming. Under pressure on four sides for 30~120 minutes, the gaps between strands are reduced to the most extent, and the shape of the slabs is fixed. Finally, the forming slabs are moved to the hot press and then are pressed to be blanks with a temperature of about 135~150°C, a pressure of 4~8 MPa and a time of 1.2~1.5 min/mm (blank thickness), as shown in Fig. 1(d).

It should be noted that the phenol formaldehyde resin used to produce ESWood is almost no harmful gases emission during processing and application. According to a certified third-party test report, formaldehyde emissions of ESWood is less than 0.1 mg/L, while 0.5 mg/L is required by the strictest provisions of Chinese national codes.

2.4 Post-Processing

After the process of hot-press forming, the blanks are dried in a kiln to equilibrium moisture content. The reason is that the moisture content is high with unbalanced distribution in the hot-press forming blanks since the blanks are relatively large and thick. The drying process not only decreases the moisture content but also balances the moisture distribution, which enhances the strength and dimension stability of the blanks.

Depending on the size requirements, these dried blanks after cutting, gluing, stacking, and compressing can finally form different structural components, as shown in Fig. 1(e). With these production processes, the ESWood components are featured by oblique strands on cross sections and an aesthetic appearance with wood texture on four sides, which enhances its decorative function. Meanwhile, the oblique strand structure with special processing technic of ESWood solves the problems of potential voids in some wood composites including PSL and thus increases the compactness and strength of final products. With better appearance and strength, ESWood can used in a wider application range, such as an engineered wood production for construction, furniture wood or decorated materials.

3 Mechanical Properties of ESWood based on Small Clear Specimen Tests

Considering the fact that ESWood is a new invention and no testing standard has been established, the standards for timber structure is referenced in this study. In Chinese timber structure design standard, small clear specimen tests are demanded for determining design values of mechanical properties of timber. In view of material characteristics and design method, it is reasonable to adopt the small clear specimen test method to obtain mechanical properties of ESWood.

In mind of comparing mechanical properties of ESWood with other engineered wood/bamboo-based products, totally 680 small clear specimens were tested to determine the tensile strength, compression strength, shearing strength, bending strength, modulus of elasticity and density of ESWood material. In each test item, the moisture content of all the specimens was tested at the end. According to the requirements of the test standards, all the strength values except for the perpendicular-to-grain tensile strength were adjusted to the reference strength values with a reference moisture content of 12% using the Eq. (1):

$$f_{12} = f_{\omega}[1 + \alpha(\omega - 12)] \tag{1}$$

where f_{12} is the strength at 12% MC; f_{w} is the strength at ω% MC; α is a conversion coefficient referred in the corresponding standards; ω is the moisture content during the test.

Since ESWood is a eucalyptus-based composite material, the definition of its direction parallel or perpendicular to grain obviously differs from that of the log. In this study, the direction along the length of the strands is defined as the direction parallel to grain (Fig. 2(a)), while direction perpendicular to the strands is defined as the direction perpendicular to grain (Fig. 2(b)). Meanwhile, glued layers are observed between the adjacent strand layers in ESWood, which may influence the compression strength and tensile strength perpendicular to grain. Hence two loading directions (Ⅰ and Ⅱ) are also defined in the tests, as shown in Fig. 2(c), Fig. 2(d).

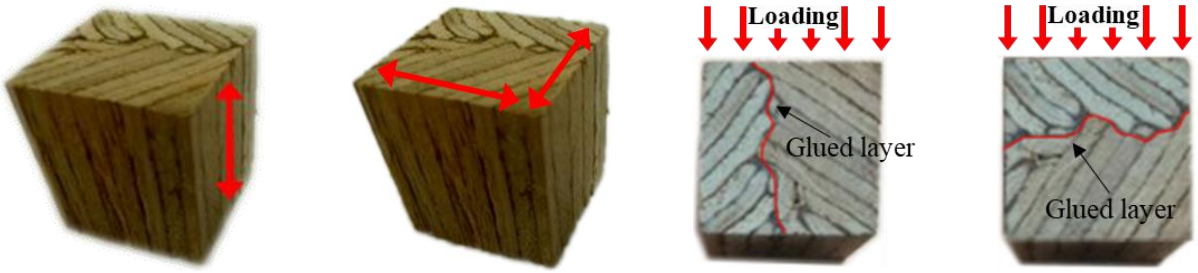

Figure 2: Definition of directions in ESWood: (a) Parallel to grain; (b) Perpendicular to grain; (c) Parallel to glued layer (Ⅰ direction); (d) Perpendicular to glued layer (Ⅱ direction)

3.1 Tension Test

3.1.1 Tension Test Parallel to Grain

Sixty specimens were tested to obtain the tensile strength parallel to grain. The geometric dimensions of the specimens are shown in Fig. 3, which were designed according to Chinese standard GB/T 1938-2009 [31]. A pair of grips were used to clamp the specimens on the universal test machine, and the tensile load was applied continuously at a rate of 1 mm/min. The parallel-to-grain tensile strength $f_t^{\parallel}$ was obtained by:

$$f_t^{\parallel} = \frac{F_{tu}^{\parallel}}{b\,t} \tag{2}$$

where $F_{tu}^{\parallel}$ is the maximum tensile load in the test; b and t are the measured dimensions of the cross section in the middle of the specimens. According to the test results, the mean tensile strength parallel to grain is 112 MPa, and the coefficient of variation (COV) is 24.8%.

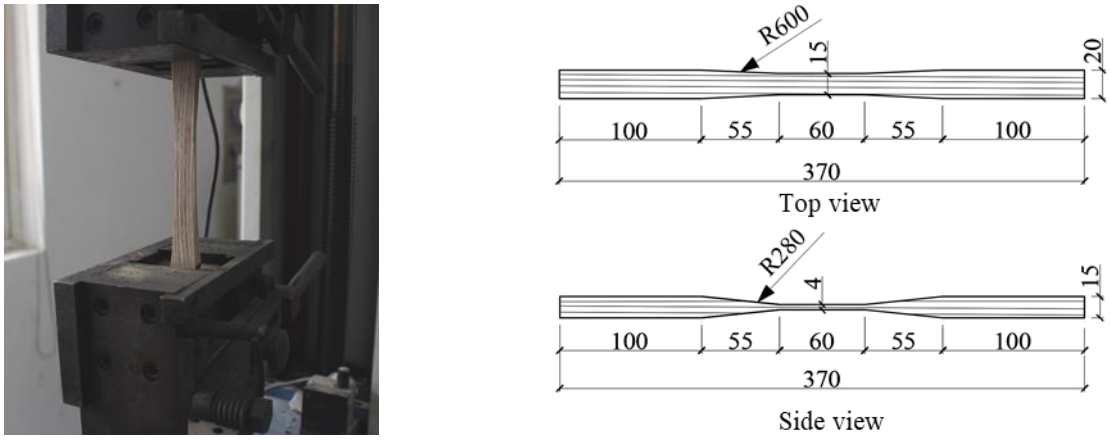

Figure 3: Test setup and specimen for parallel-to-grain tensile strength tests (unit: mm)

The tests showed that all the specimens behaved in an elasto-brittle manner. The main reason is that the tensile stress is mainly carried by the fibers due to their higher stiffness and strength compared to those of glue, and thus the damage is significantly attributed to the breakage of fibers. With the brittle behavior of the fibers, the parallel-to-grain tensile failure shows high strength with brittleness.

As illustrated in Fig. 4(a), the ESWood material exhibits a bilinear behavior before failure. Rupture failure occurred in the center part of most specimens, followed by a sudden loss of load-carrying capacity. Two kinds of fracture surfaces (i.e., diagonal fracture surface and flat surface) were observed, as shown in

Figs. 4(b), 4(c). It should be mentioned that no obvious difference of test results was found between the two failure modes.

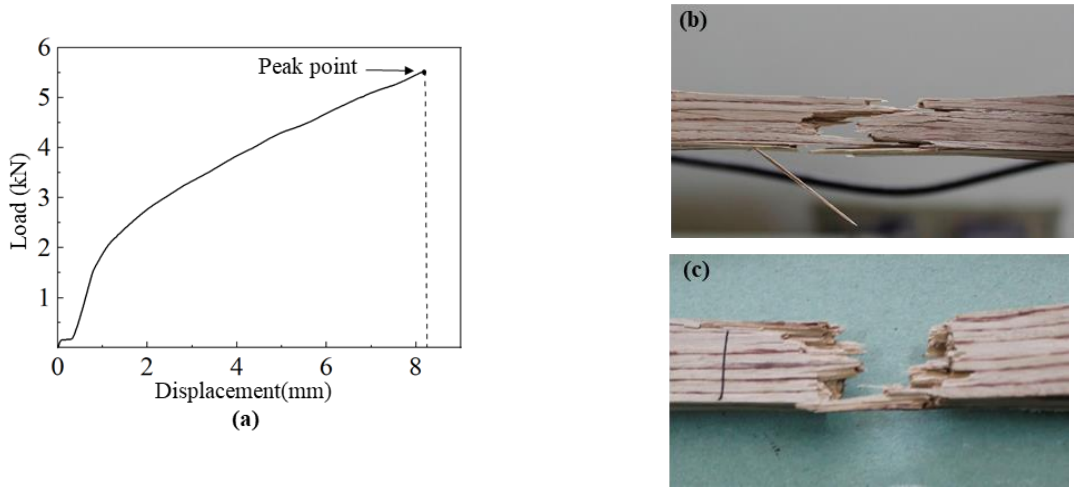

Figure 4: Parallel-to-grain tensile test results: (a) typical load-displacement curve; (b) rupture failure with a diagonal fracture surface; (c) rupture failure with a flat fracture surface

3.1.2 Tension Test Perpendicular to Grain

The geometric configuration of the specimens for perpendicular-to-grain tensile strength test is illustrated in Fig. 5. The specimens were designed based on ASTM D143-2014 [32] because currently there are no available Chinese standards. Totally 120 specimens were tested, in which 60 specimens were loaded parallel to glued layer (i.e., in direction Ⅰ) and the others were loaded perpendicular to glued layer (i.e., in direction Ⅱ), which can be seen in Fig. 5. The tensile load was applied continuously by the universal test machine at a rate of 0.5 mm/min. The perpendicular-to-grain tensile strength $f_{t,I}^{\perp}$ (loading in direction Ⅰ) and $f_{t,II}^{\perp}$ (loading in direction Ⅱ) were obtained by:

$$f_{t,I}^{\perp} = f_{t,II}^{\perp} = \frac{F_{tu}^{\perp}}{bt} \tag{3}$$

where $F_{tu}^{\perp}$ is the ultimate tensile load in the test; b and t are the measured dimensions of the cross section in the middle of the specimens. The mean perpendicular-to-grain tensile strengths in direction Ⅰ and direction Ⅱ are 2.34 MPa and 3.00 MPa, respectively. The corresponding variation coefficients are 21.7% and 22.6%, respectively.

Typical failure mode of the specimens for the perpendicular-to-grain tensile test was presented in Fig. 6. The elasto-brittle manner was also observed in the tests with loading in either direction Ⅰ or direction Ⅱ, with a crack running through the entire cross section. Although the failure mode is the same between the specimens loading in direction Ⅰ and that loading in direction Ⅱ, however, the mean value of perpendicular-to-grain tensile strength in direction Ⅱ is 28% larger than that in direction Ⅰ, which indicates that the glued layer has a significant influence on the perpendicular-to-grain tensile strength of ESWood.

In this case, tensile stresses are transmitted via fibers and glue. Because the tensile strength of fibers is much larger than that of glue, the damage firstly occurs in the glue lines, and the failure is mainly attributed to the fracture of the glue. On the minimum cross section, the glue area of specimens loading in direction Ⅱ is smaller than that loading in direction Ⅰ due to the glued layer, hence the tensile strength in direction Ⅱ is larger than that in direction Ⅰ.

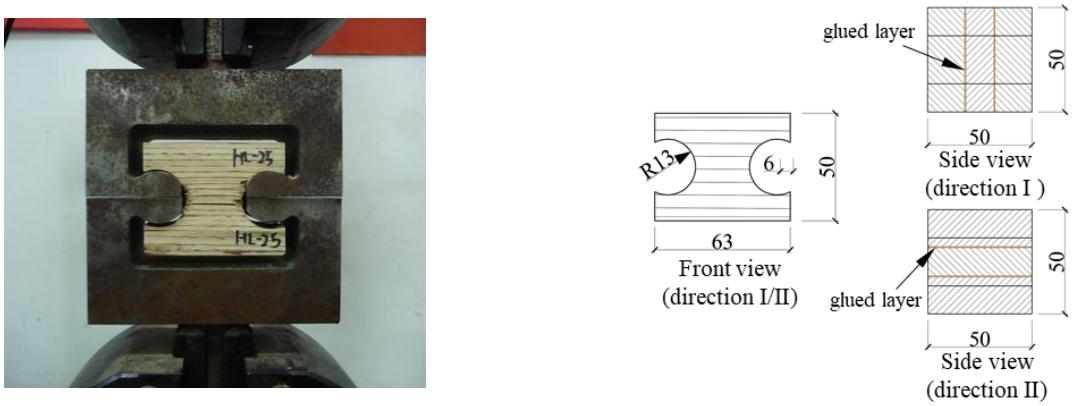

Figure 5: Test setup and specimen for perpendicular-to-grain tensile strength tests in direction Ⅰ and Ⅱ (unit: mm)

Figure 6: Typical failure mode of specimens in perpendicular-to-grain tensile tests

3.2 Compression Test

3.2.1 Compression Test Parallel to Grain

The perpendicular-to-grain compression test was conducted on a universal test machine with an ultimate capacity of 50 kN, as shown in Fig. 7(a). According to Chinese standard GB/T 1935-2009 [33] and GB/T 15777-2017 [34], sixty specimens with the dimension of 20 × 20 × 30 mm were prepared for testing strength, while sixty specimens with the dimension of 20 × 20 × 60 mm were prepared for testing MOE. Compression load was applied continuously at a rate of 0.5 mm/min. The compression strength and MOE parallel to grain were calculated by:

$$f_c^{\parallel} = \frac{F_{cp}^{\parallel}}{w\,d}, \quad E_c^{\parallel} = \frac{\Delta F_c^{\parallel}}{w\,d\,\Delta \varepsilon_c^{\parallel}} \tag{4}$$

where $F_{cp}^{\parallel}$ is the peak compression load applied on the specimens; w and d are the measured dimensions of the cross section; $\Delta F_c^{\parallel}$ and $\Delta \varepsilon_c^{\parallel}$ are compression load increment and strain increment within the linear elastic stage. The mean compressive strength parallel to grain is obtained as 67 MPa, and the MOE is obtained as 16472 MPa. The variation coefficients for compressive strength and MOE are 9.5% and 8.7%, respectively, which indicates excellent stability of the results.

A typical stress-strain curve and two dominating failure modes of the specimens are demonstrated in Fig. 8. The load-carrying capacity of fiber in compression is significantly affected by the stiffness and strength of the surrounding glue, which restricts the transverse deformation of fibers [35]. Before the proportional limit, the specimen was in linear elastic stage. As the load increased beyond the proportional

limit, the damage mainly occurred in glue or in the fiber-glue interface, resulting in debonding. Buckling and kinking of fibers due to compression would cause more serious damage in the interface, and thus the specimen was consequently failed due to local buckling of the fibers with crushing. In the test, crushing failure was observed in most of the specimens as shown in Fig. 8(b), while in a few specimens, strands were separated from each other along the glued lines, as shown in Fig. 8(c). Moreover, a ductile post-yielding behavior was observed from the stress-strain curve.

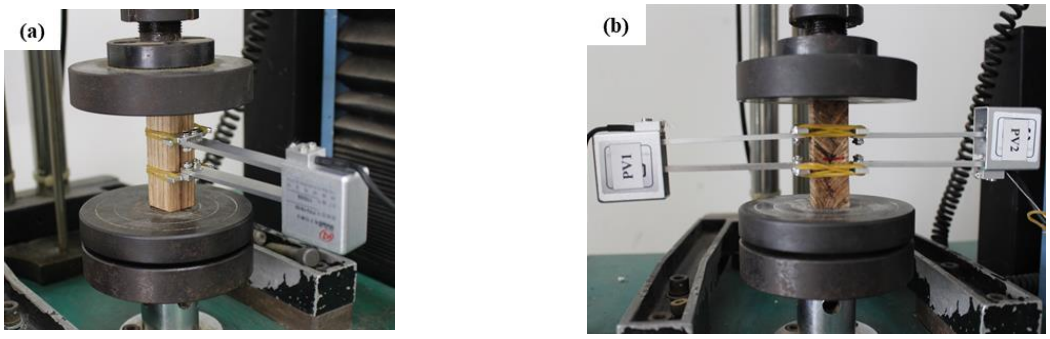

Figure 7: Setup for compression test: (a) parallel-to-grain MOE test; (b) perpendicular-to-grain MOE test

Figure 8: Parallel-to-grain compression test results: (a) typical stress-strain curve; (b) crushing failure; (c) failure with strands separated along the glued lines

3.2.2 Compression Test Perpendicular to Grain

Perpendicular-to-grain compression tests for determining the strength and MOE were conducted according to Chinese standard GB/T 1939-2009 [36] and GB/T 1943-2009 [37], respectively. One hundred twenty specimens with the dimension of 20 × 20 × 30 mm were prepared for the strength test while 120 specimens with the dimension of 20 × 20 × 60 mm were prepared for the MOE test. Half specimens were loaded in parallel to glued layer (direction Ⅰ), and the others were loaded in perpendicular to the glued layer (direction Ⅱ). Compression load was applied at a rate of 0.5 mm/min using the universal test machine, as shown in Fig. 7(b). The compression strength and MOE perpendicular to grain were calculated by:

$$f_{c,I}^{\perp} = f_{c,II}^{\perp} = \frac{F_{cpl}^{\perp}}{w\,d}, \quad E_{c,I}^{\perp} = E_{c,II}^{\perp} = \frac{\Delta F_{c}^{\perp}}{w\,d\,\Delta\varepsilon_{c}^{\perp}} \tag{5}$$

where $F_{cpl}^{\perp}$ is the proportional limit compression load applied on the specimens; w and d are the measured dimensions of the cross section; $\Delta F_{c}^{\perp}$ and $\Delta\varepsilon_{c}^{\perp}$ are compression load increment and strain increment within the linear elastic stage. The average compressive strengths perpendicular to grain are obtained as

4.77 MPa (direction Ⅰ) and 3.68 MPa (direction Ⅱ), with variation coefficients of 22.8% and 20.3%, respectively. The average perpendicular-to-grain MOE is obtained as 843 MPa (direction Ⅰ) and 532 MPa (direction Ⅱ), with variation coefficients of 16.4% and 22.2%, respectively.

The typical load-deformation curve and failure modes of the specimens under perpendicular-to-grain force are shown in Fig. 9. The point of proportional limit was automatically identified by the software of the universal test machine. The proportional limit in direction Ⅰ is much larger than that in the direction Ⅱ, as shown in Fig. 9(a). Although the point of proportional limit, instead of the point of ultimate limit, was adopted for determining the perpendicular-to-grain compressive strength, the specimens in strength tests were loaded until failures occurred. For the specimens loaded in direction Ⅰ, failure usually occurred along the glued line between two strands and the glued layer, as shown in Fig. 9(b). However, for specimens loaded in direction Ⅱ, failure generally occurred along the glued line between two strands, as shown in Fig. 9(c). Both the compressive strength and modulus in the direction Ⅱ are lower than those in direction Ⅰ.

When specimens were subjected to perpendicular-to-grain compression, fibers acted as reinforcements by which the transverse deformations of the glue were restrained, resulting in the glue in a 2-axial compressive stress state. Hence the dominant yield maximum shear stress in the plane with an angle of 45° to normal stress caused cracks in the glue or in the fiber-glue interface, which then developed along the fibers and finally formed a failure surface.

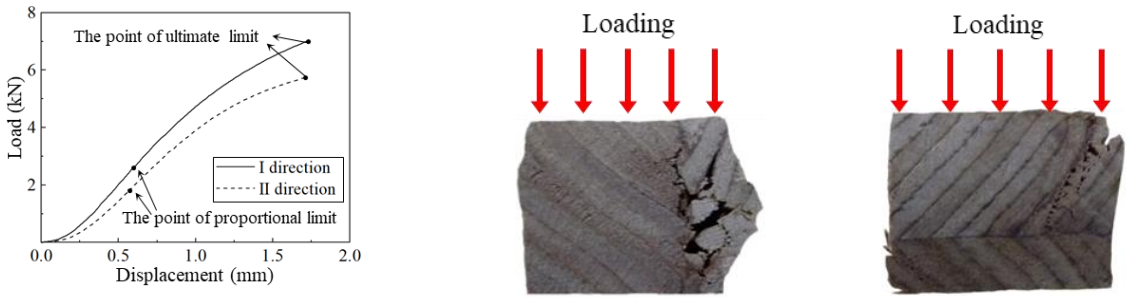

Figure 9: Perpendicular-to-grain compression test results: (a) typical load-deformation curve; (b) failure along glued layer in specimens loaded in direction Ⅰ; (c) failure along the glued line in specimens loaded in direction Ⅱ

3.3 Shear Test

The shear test was conducted according to Chinese standard GB/T 1937-2009 [38]. The geometric configuration of the specimens for the test is presented in Fig. 10(a). The specimens were hold using the clamping fixture designed by the authors. The loading rate was set at 0.6 mm/min, and the shear force was applied across the thickness direction of the specimen in the cutting plane to induce shear deformation, as shown in Fig. 10(b). The shear strength f_s was obtained by:

$$f_s^{\parallel} = \frac{0.96 F_{sp}^{\parallel}}{b l} \tag{6}$$

where $F_{sp}^{\parallel}$ is the peak shearing force applied on the specimens; b and l are the measured dimensions of the shear plane. The test results presented that the average value of shearing strength parallel to grain is 11.83 MPa, with a variation coefficient of 17.1%.

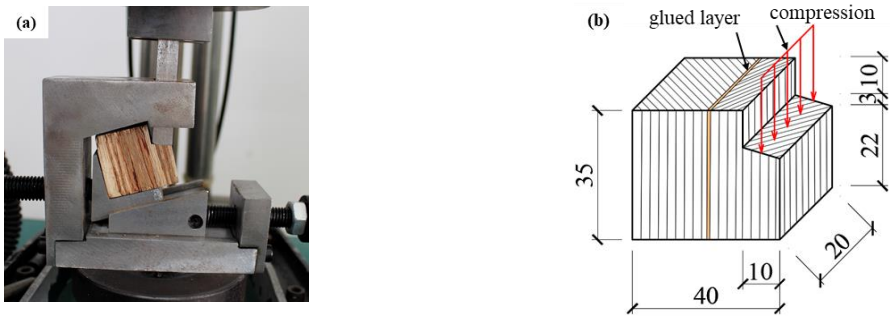

Figure 10: Shear test: (a) setup; (b) specimen geometry

The shear failure mode was almost the same among all the specimens. During the test, fibers crossed the shearing plane gradually broken as the force increased, and consequently, the specimens were split into two parts along the shear plane with rough failure surface, as shown in Fig. 11.

Figure 11: Typical failure mode of specimens in shear tests

3.4 Bending Test

The bending test was conducted based on Chinese standard GB/T 1936-2009 [39]. Sixty specimens with the size of 20 × 20 × 300 mm were tested. The longitudinal direction of the specimen is along the length direction of strands. As shown in Fig. 12, the test setup includes loading bearings with a 30 mm radius of curvature. The load was applied in the middle of the specimen using the loader of radius 30 mm, at the rate of 5.0 mm/min. The bending strength f_b was calculated by:

$$f_b = \frac{3F_{bp}l}{2bh^2} \tag{7}$$

where F_{bp} is the peak force corresponding to the ultimate load-carrying capacity of the specimens; l is the supporting length; b and h are the measured cross sectional dimensions of the specimens. It was found that the mean value of bending strength is 111 MPa, with a variation coefficient of 10.0%.

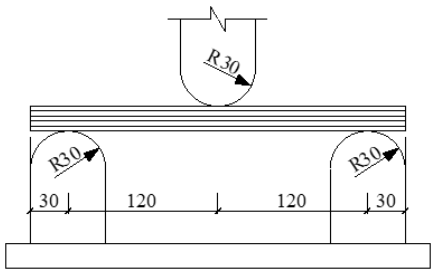

Figure 12: Test setup of bending test

A typical load-deflection curve and two failure modes of bending specimens are presented in Fig. 13. For the bending behavior, a linear elastic range was initially observed and then the slope of the load-deflection curve decreased as the tension failure of the bottom strands gradually occurred, as demonstrated in Fig. 13(a). On further loading, two typical failure modes were observed: one is the splitting with cracks along the glued line, as shown in Fig. 13(b), and the other is the tensile failure of more strand fibers, which is extended from the bottom to the middle, as shown in Fig. 13(c). Due to the high strength and stiffness with brittle behavior of the fibers, the flexural failure showed high strength without ductility.

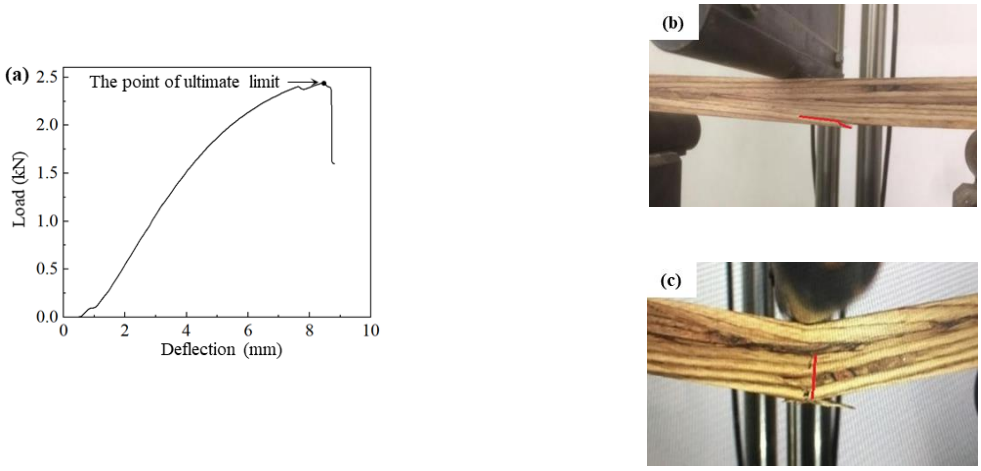

Figure 13: Bending test results: (a) typical load-deflection curve; (b) splitting failure; (c) tensile failure

3.5 Comparison with Other Wood/Bamboo-Based Materials

Twenty specimens with dimensions of 20 × 20 × 20 mm were tested according to Chinese standard GB/T 1933-2009 [40] for determining the density of ESWood material. Oven drying method was adopted. The average density of ESWood is 864 kg/m^3 with a variation coefficient of 9.2%, which is relatively larger than that of general wood material.

The other main mechanical properties obtained from the tests are listed in Tab. 1. From the results presented herein, it appears that in the longitudinal direction, the tensile strength is 1.7 times that of compressive strength, while in the transverse direction, the compressive strength is 2.0 times and 1.2 times that of tensile strength in the direction Ⅰ and direction Ⅱ, respectively. Besides, for both tension and compression tests, the perpendicular-to-grain strength values are much smaller than the parallel-to-grain strength values. Meanwhile, it is worth noting that the glued layer has a significant influence on the mechanical perpendicular-to-grain properties of ESWood, since the difference of tensile strength, compression strength and compression MOE between the direction Ⅰ and direction Ⅱ is 28%, 23%, and 37%, respectively.

However, it should also be mentioned that the adoption of high pressure in the production process makes the adjacent slabs or blanks to be well embedded and glued with each other and thus guarantees the reliability of the bonding performance and dimension stability in a certain extent, despite the bonding interface is relatively irregular. From the above test results, the oblique bonding interface seems to have little influence on the bonding performance.

Comparisons of mechanical properties of ESWood with Sitka spruce [41], Douglas-fir LVL [42], Parawood OSL [24], Spruce-pine-fir (SPF) Glulam [43] and laminated bamboo (Glubam) [44] are concluded in Tab. 2. In the parallel-to-grain direction, both the compressive strength and tensile strength of ESWood obviously surpass the other five wood/bamboo-based products. In the perpendicular-to-grain direction, it is noted that the tensile strength of ESWood is close to that of Douglas-fir LVL, but is approximately twice the value of that of SPF Glulam. Shear strength of ESWood is also larger than that of

other materials. Meanwhile, ESWood also has a considerably larger flexural strength than the other five products. The flexural strength of ESWood is 11% larger than that of Glubam, and is up to 3.5 times that of SPF Glulam. Considering the ratio of flexural strength to density, the value of ESWood is lower than that of Sitka spruce, but it is similar to or larger than that of the other four products.

Table 1: Main mechanical properties of ESWood

Category	Direction of loading	Strength (MPa)			MOE (MPa)	
		Mean	COV (%)	5-percentile	Mean	COV (%)
Tension	Parallel to grain	112	24.8	66.3	-	-
	perpendicular to grain (Ⅰ)	2.34	21.7	1.5	-	-
	perpendicular to grain (Ⅱ)	3.00	22.6	1.9	-	-
Compression	parallel to grain	67	9.5	56.5	16472	8.7
	perpendicular to grain (Ⅰ)	4.77	22.8	3.0	843	16.4
	perpendicular to grain (Ⅱ)	3.68	20.3	2.5	532	22.2
Shear	Parallel to grain	11.83	17.1	8.5	-	-
Flexure	-	111	10.0	92.7	-	-

Note: Both the strength values and MOE values are the reference values with a moisture content of 12%

Table 2: Mechanical properties of ESWood and other wood/bamboo-based materials

Products	Density	Compression	Tension			Shear	Flexure	
	ρ (kg/m^3)	$f_c^{\parallel}$ (MPa)	$f_t^{\parallel}$ (MPa)	$f_t^{\perp}$ (MPa)		$f_s^{\parallel}$ (MPa)	f_b (MPa)	f_b / ρ (10^4 m^{2}s^{-2})
				$f_{t,I}^{\perp}$	$f_{t,II}^{\perp}$			
ESWood	864	67	112	2.3	3.0	12.0	111	12.8
Sitka spruce [40]	383	36	59	-		9.0	67	17.5
Douglas-fir LVL [41]	520	57	55	2.3		11.0	68	13.1
Parawood OSL [24]	700	39	36	-		4.1	61	8.7
SPF Glulam [42]	408	28	-	1.2		3.5	32	7.8
Glubam [43]	800-980	51	82	-		7.2	99	10.1-12.4

Comparisons of selected mechanical properties of ESWood with those of solid eucalyptus and eucalyptus-based LVL are also concluded. Density, parallel-to-grain compressive strength, shear strength and static flexural strength of ESWood, solid eucalyptus tested by Castro [17] and R. Wagenführ [19], and LVL products tested by Aydin [12] and Palma [45] are shown in Tab. 3. It is found that the selected mechanical properties of ESWood are significantly larger than those of other eucalyptus-based materials. To be specific, the parallel-to-grain compressive strength of ESWood is almost 40% and 23% larger than that of solid eucalyptus and LVL. The shear strength of ESWood is twice the value of LVL and is 20% larger than that of the two types of solid eucalyptus. Moreover, ESWood also has a considerably larger flexural strength than solid eucalyptus and LVL products.

Table 3: Selected mechanical properties of ESWood and comparable eucalyptus-based materials

Species/products	Density ρ (kg/m^3)	Compression $f_c^{\parallel}$ (MPa)	Shear $f_s^{\parallel}$ (MPa)	Flexure f_b (MPa)
ESWood	864	67	12	111
Solid eucalyptus 1 [17]	539	41.4	9	86
Solid eucalyptus 2 [19]	800	44	9.5	89.5
LVL 1[12]	674	51.7	-	94.9
LVL 2[44]	690	58	6	89

From the results presented herein, it appears that ESWood has larger strength values in almost all mechanical properties, which is mainly attributed to the confinement of fibers. There are strong reasons to consider that ESWood is able to serve as a promising alternative for existing wood/bamboo-based composite materials for structural applications.

4 Performance of Full-scale ESWood Beams in Flexure

According to the small clear specimen test results, one of the most potential structural uses of ESWood is as structural beams since ESWood material has a high flexural strength to weight ratio. In order to observe the performance of structural beams made of ESWood, an experimental study on the mechanical behavior of ESWood beams was also conducted. Several important component-level mechanical parameters of beams were obtained.

4.1 Tests of ESWood Beam in Flexure

Two full-scale beams with the size of 180 × 230 × 4480 mm were tested to observe the mechanical performance of ESWood beams. The load configurations were in accordance with GB/T 50329-2012 [46], which recommended a four-point bending with a span of 18 times the depth for bending strength and stiffness determination, as shown in Fig. 14. The distance between two loading points was 1800 mm while the distance between loading point and the central line of supports was 1200 mm. During the tests, the beams were simply supported, and the loads were applied using a servo-hydraulic test machine which was fixed to the reaction frame. Five linear variable differential transformers (LVDTs) were arranged at different positions of the specimens for the deflection measurement.

The tests were conducted in two stages. Initially, the load was applied continuously up to the upper limit (i.e., 30% of the ultimate load-carrying capacity of the specimen) at a rate of 6.0 mm/min and then unloaded to the lower limit (i.e., 10% of the ultimate load-carrying capacity) with the same rate, which was repeated for five times. Then the load was applied up to the ultimate load-carrying capacity of the specimen at a constant rate of 8.0 mm/min.

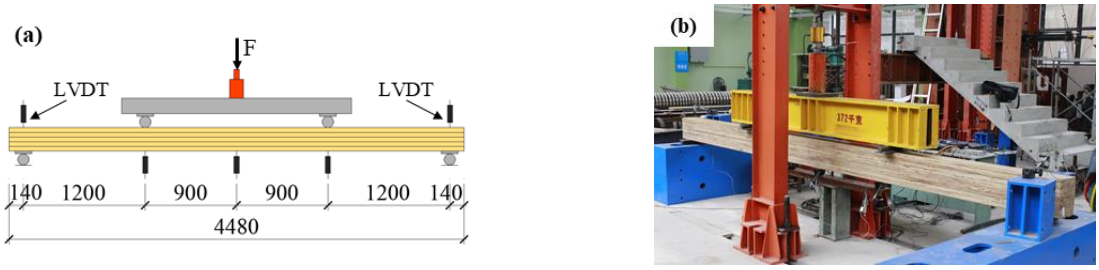

Figure 14: Bending test: (a) load configuration; (b) test setup

The failure mode was the same between the two specimens. As the load increasing, tension failure of the bottom strands initially occurred in the middle of the beam, as shown in Fig. 15(a). On further loading, more strands failed in tension and then cracks quickly extended along the glued lines between some strands up to the maximum load-carrying capacity, as shown in Fig. 15(b). This failure mode was similar to that of the small clear specimens in the bending tests.

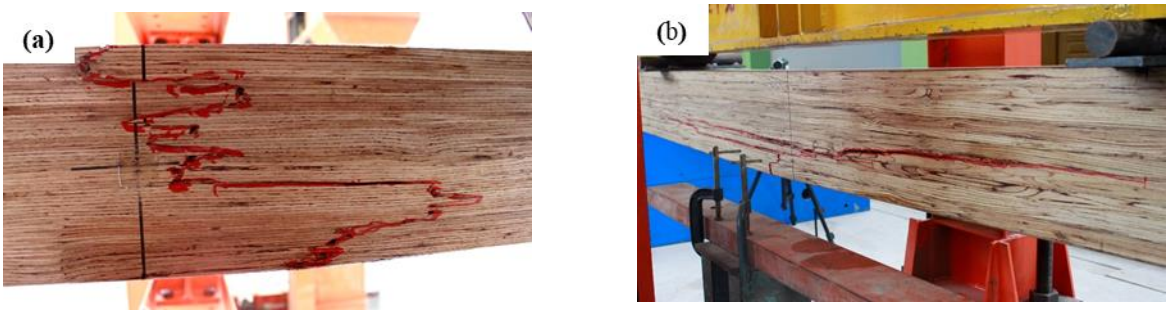

Figure 15: Failure mode of ESWood beams: (a) tension failure of bottom strands (bottom surface); (b) cracks along the glued lines (side face)

Three mechanical properties were obtained via the bending test, including local (shear-free) MOE $E_{m,l}$, global MOE $E_{m,g}$ and bending strength $f_m^{'}$, which were calculated by Eq. (8), Eq. (9) and Eq. (10), respectively.

$$E_{m,l} = \frac{a l_0^2 \Delta F}{16 I \Delta \omega} \tag{8}$$

$$E_{m,g} = \frac{a \Delta F}{48 I \Delta \omega}(3l_0^2 - 4a^2) \tag{9}$$

$$f_m^{'} = \frac{a F_u}{2W} \tag{10}$$

where a is the distance between loading point and the nearest support; l_0 is the distance between two loading points; I is the second moment of area of the beam; ΔF is an increment of load between the upper limit and lower limit; $\Delta \omega$ is the increment of deformation corresponding to ΔF; F_u is the maximum load; W is the section modulus. As shown in Fig. 16 and Tab. 4, all the beams behaved in an elasto-brittle manner with a mean bending strength value of 89 MPa. However, the deflection corresponding to the maximum load was larger than 80 mm (i.e., one-fiftieth of beam's span), indicating great deformation capacity of the ESWood beam. Moreover, both the local MOE and global MOE of the tested beams were similar, and the mean values of those were 13047 MPa and 12771 MPa, respectively.

Table 4: Results obtained from bending tests

Specimen No.	Max. load F_u (kN)	Bending strength $f_m^{'}$ (MPa)	Local MOE $E_{m,l}$ (MPa)	Global MOE $E_{m,g}$ (MPa)
B-1	133	91	12869	12598
B-2	136	86	13225	12944

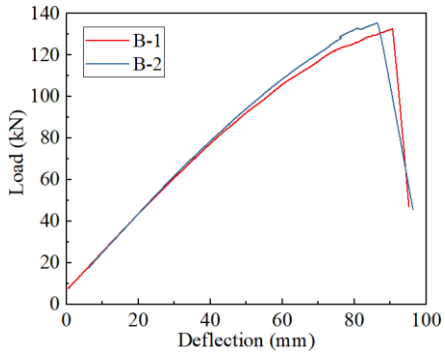

Figure 16: Load-deflection curve of specimens in bending tests

4.2 Comparison with Small Clear Specimen Tests

According to the test results, it is noted that the mean flexural strength obtained from the full-scale component tests is lower than that obtained from small clear specimen tests. It is a normal phenomenon in wood and wood-based materials because of the well-known size effect of wood. The equation proposed by Fonselius [47] is commonly used to calculate the size effect on strength for wood composite materials like laminated veneer lumber, and the strength of ESWood obtained from the full-scale test is approximately 17% larger than the theoretical values calculated by the equation, which indicates that the size effect of ESWood is lower than the average level. Moreover, the mechanical performance of full-scale beams is satisfactorily stable since the test results of two specimens in the bending test are very close.

With desirable strength and MOE values, the ESWood material has real potential as a promising alternative for existing wood/bamboo-based composite materials in building constructions. Furthermore, it is quite beneficial to the natural forests and building industries with the utilization of fast-growing small diameter eucalyptus wood for manufacturing ESWood because of its low price, sustainability, and renewability.

5 Conclusion

ESWood is produced through raw eucalyptus selection, making veneer strands, gluing and pressing, and post-processing. Adopting this manufacturing technique, ESWood is featured by oblique strands on cross sections and an aesthetic appearance with wood texture on four sides, which is quite different from existing structural composite lumber products. After a series of small clear specimen tests and full-scale beams tests, ESWood showed a better mechanical performance in comparison with other engineered wood/bamboo-based products. According to the test results and comparisons, the following conclusions can be summarized,

1. Results from the clear specimen tests indicate that strength and stiffness properties of ESWood are significantly affected by grain directionality and glued layers.

2. The compressive strength and tensile strength of ESWood are up to 2.4 times and 3.1 times that of other selected products respectively, while the shear strength and flexural strength of ESWood are up to 3.5 times that of other selected products, indicating that ESWood is suitable to be used as a promising building material.

3. The size effect of ESWood is lower than the average level since the strength of ESWood obtained from full-scale bending tests is approximately 17% larger than the theoretical value.

4. The full-scale bending tests also show that beams made by ESWood have stable mechanical performance since the results are almost identical, which further provides confidence in the structural usage of ESWood.

Acknowledgement: This paper is funded by the Application for Collaborative Research Project under International Joint Research Laboratory of Earthquake Engineering (TMGFXK-2015-002-2) and Fundamental Research Funds for the Central University (22120180315, 22120170521). Moreover, Shenzhen Plantation Material Technology Co., Ltd. is gratefully acknowledged for the ESWood supplying.

References

1. He, M. J., Zhang, J., Li, Z., Li, M. L. (2016). Production and mechanical performance of scrimber composite manufactured from poplar wood for structural applications. *Journal of Wood Science, 62(5),* 429-440.
2. Kong, L. L., Zhao, Z. J., He, Z. B., Yi, S. L. (2018). Development of schedule to steaming prior to drying and its effects on Eucalyptus grandis × E. urophylla wood. *European Journal of Wood and Wood Products, 76(2),* 591-600.
3. Acosta, M. S., Mastrandrea, C., Lima, J. T. (2008). Wood technologies and uses of Eucalyptus wood from fast grown plantations for solid products. *Proceedings of the 51st International Convention of Society of Wood Science and Technology*, 10-12.
4. Esteves, B., Marques, A. V., Domingos, I., Pereira, H. (2007). Influence of steam heating on the properties of pine (Pinus pinaster) and eucalypt (Eucalyptus globulus) wood. *Wood Science and Technology, 41(3),* 193-207.
5. Li, H. T., Wu, G., Zhang, Q. S., Deeks, A. J., Su, J. W. (2018). Ultimate bending capacity evaluation of laminated bamboo lumber beams. *Construction and Building Materials, 160,* 365-375.
6. Tazi, M., Erchiqui, F., Kaddami, H., Bouazara, M., Poaty, B. (2015). Evaluation of mechanical properties and durability performance of HDPE-wood composites. *Journal of Renewable Materials, 2(4),* 258-263.
7. Maloney, T. M. (1993). *Modern particleboard and dry-process fiberboard manufacturing*. San Francisco: Miller Freeman Inc.
8. Çolak, S., Çolakoğlu, G., Aydin, I., Kalaycioğlu, H. (2007). Effects of steaming process on some properties of eucalyptus particleboard bonded with UF and MUF adhesives. *Building and Environment, 42(1),* 304-309.
9. Pan, Z. L., Zheng, Y., Zhang, R. H., Jenkins, B. M. (2007). Physical properties of thin particleboard made from saline eucalyptus. *Industrial Crops and Products, 26(2),* 185-194.
10. Ashori, A., Nourbakhsh, A. (2008). Effect of press cycle time and resin content on physical and mechanical properties of particleboard panels made from the underutilized low-quality raw materials. *Industrial Crops and Products, 28(2),* 225-230.
11. Gaunt, D., Penellum, B., McKenzie, H. M. (2003). Eucalyptus nitens laminated veneer lumber structural properties. *New Zealand Journal of Forestry Science, 33(1),* 114-125.
12. Aydın, İ., Çolak, S., Çolakoğlu, G., Salih, E. (2004). A comparative study on some physical and mechanical properties of laminated veneer lumber (LVL) produced from Beech (Fagus orientalis Lipsky) and Eucalyptus (Eucalyptus camaldulensis Dehn.) veneers. *Holz Als Roh-Und Werkstoff, 62(3),* 218-220.
13. Saviana, J., Zitto, S., Piter, J. C. (2009). Bending strength and stiffness of structural laminated veneer lumber manufactured from fast-growing Argentinean Eucalyptus grandis. *Maderas. Cienciay Tecnología, 11(3),* 183-190.
14. Bal, B. C., Bektaş, İ. (2012). The effects of wood species, load direction, and adhesives on bending properties of laminated veneer lumber. *BioResources, 7(3),* 3104-3112.
15. Bal, B. C., Bektaş, İ. (2012). The effects of some factors on the impact bending strength of laminated veneer lumber. *BioResources, 7(4),* 5855-5863.
16. Bal, B. C. (2016). Some technological properties of laminated veneer lumber produced with fast-growing Poplar and Eucalyptus. *Maderas. Ciencia y Tecnología, 18(3),* 413-424.
17. Castro, G., Paganini, F. (2003). Mixed glued laminated timber of poplar and Eucalyptus grandis clones. *Holz Als Roh-Und Werkstoff, 61(4),* 291-298.
18. Piter, J. C., Cotrina, A. D., Zitto, M. S., Stefani, P. M., Torrán, E. A. (2007). Determination of characteristic strength and stiffness values in glued laminated beams of Argentinean Eucalyptus grandis according to European standards. *Holz Als Roh-Und Werkstoff, 65(4),* 261-266.
19. Franke, S., Marto, J. (2014). Investigation of Eucalyptus globulus wood for the use as an engineered material. *World Conference on Timber Engineering*, 2014.

20. Lara-Bocanegra, A. J., Majano-Majano, A., Crespo, J., Guaita, M. (2017). Finger-jointed Eucalyptus globulus with 1C-PUR adhesive for high performance engineered laminated products. *Construction and Building Materials, 135,* 529-537.
21. Liao, Y. C., Tu, D. Y., Zhou, J. H., Zhou, H. B., Yun, H. et al. (2017). Feasibility of manufacturing cross-laminated timber using fast-grown small diameter eucalyptus lumbers. *Construction and Building Materials, 132,* 508-515.
22. Lu, Z. H., Zhou, H. B., Liao, Y. C., Hu, C. S. (2018). Effects of surface treatment and adhesives on bond performance and mechanical properties of cross-laminated timber (CLT) made from small diameter Eucalyptus timber. *Construction & Building Materials, 161,* 9-15.
23. Chirasatitsin, S., Prasertsan, S., Wisutmethangoon, W., Kyokong, B. (2005). Mechanical properties of rubberwood oriented strand lumber (OSL): the effect of strand length. *Songklanakarin Journal of Science and Technology, 27(5),* 1047-1055.
24. Chotchuay, V., Kyokong, B., Ouypornprasert, W. (2008). Strength and reliability of oriented strand lumber made from heat-treated parawood strands. *Sonklanakarin Journal of Science and Technology, 30(5), 64*9.
25. Bayatkashkoli, A., Faegh, M. (2014). Evaluation of mechanical properties of laminated strand lumber and oriented strand lumber made from Poplar wood (Populus deltoides) and Paulownia (Paulownia fortunei) with urea formaldehyde adhesive containing nanoclay. *International Wood Products Journal, 5(4), 19*2-195.
26. Malanit, P., Barbu, M. C., Frühwald, A. (2011). Physical and mechanical properties of oriented strand lumber made from an Asian bamboo (Dendrocalamus asper Backer). *European Journal of Wood and Wood Products, 69(1), 27*-36.
27. De Souza, F., Del Menezzi, C. H. S., Bortoletto Júnior, G. (2011). Material properties and nondestructive evaluation of laminated veneer lumber (LVL) made from Pinus oocarpa and P. kesiya. *European Journal of Wood and Wood Products, 69(2),* 183-192.
28. Çolak, S., Aydin, I., Demirkir, C., Çolakoğlu, G. (2004). Some technological properties of laminated veneer lumber manufactured from pine (Pinus sylvestris L.) veneers with melamine added-UF resins. *Turkish Journal of Agriculture and Forestry, 28(2),* 109-113.
29. Kurt, R., Cavus, V. (2011). Manufacturing of parallel strand lumber (PSL) from rotary peeled hybrid poplar I-214 veneers with phenol formaldehyde and urea formaldehyde adhesives. *Wood Research (Bratislava), 56(1),* 137-144.
30. Kurt, R., Aslan, K., Cil, M., Cavus, V. (2012). Properties of parallel strand lumber from two hybrid poplar clones using melamine urea formaldehyde adhesive. *BioResources, 7(3), 3*711-3719.
31. GB/T 1938-2009 (2009). *Method of testing in tensile strength parallel to grain of wood*. China National Standard. Beijing: Standards Press of China.
32. ASTM D143-14 (2014). *Standard test methods for small clear specimens of timber*. West Conshohocken: American Society for Testing Material Standard.
33. GB/T 1935-2009 (2009). *Method of testing in compressive strength parallel to grain of wood*. China National Standard. Beijing: Standards Press of China.
34. GB/T 15777-2017 (2017). *Method for determination of the modulus of elasticity in compression parallel to grain of wood*. China National Standard. Beijing: Standards Press of China.
35. Huang, D. S., Bian, Y. L., Zhou, A. P., Sheng, B. L. (2015). Experimental study on stress-strain relationships and failure mechanisms of parallel strand bamboo made from phyllostachys. *Construction and Building Materials, 77, 1*30-138.
36. GB/T 1939-2009 (2009). *Method of testing in compression strength perpendicular to grain of wood*. China National Standard. Beijing: Standards Press of China.
37. GB/T 1943-2009 (2009). *Method for determination of the modulus of elasticity in compression perpendicular to grain of wood*. China National Standard. Beijing: Standards Press of China.
38. GB/T 1937-2009 (2009). *Method of testing in shearing strength parallel to grain of wood*. China National Standard. Beijing: Standards Press of China.
39. GB/T 1936.1-2009 (2009). *Method of testing in bending strength of wood*. China National Standard. Beijing: Standards Press of China.

40. GB/T 1933-2009 (2009). *Method for determination of the density of wood*. China National Standard. Beijing: Standards Press of China.
41. Kretschmann, D. E. (2010). *Wood handbook, chapter 05: mechanical properties of wood*. Madison, Wisconsin, USA: Forest Products Laboratory, Department of Agriculture Forest Service.
42. Clouston, P., Lam, F., Barrett, J. D. (1998). Incorporating size effects in the Tsai-Wu strength theory for Douglas-fir laminated veneer. *Wood Science and Technology, 32(3), 2*15-226.
43. Liu, H. F., He, M. J. (2015). Effects of self-tapping screw on performance of glulam beam-to-column connections. *Journal of Building Structures, 36(7),* 126-134.
44. Xiao, Y., Yang, R. Z., Shan, B. (2013). Production, environmental impact and mechanical properties of glubam. *Construction and Building Materials, 44, 7*65-773.
45. Palma, H. A. L., Ballarin, A. W. (2011). Physical and mechanical properties of LVL panels made from Eucalyptus grandis. *Ciência Florestal, 21(3), 5*59-566.
46. GB/T 50329-2012 (2012). *Standard for test methods of timber structures*. China National Standard. Beijing: China Architecture & Building Press.
47. Fonselius, M. (1997). Effect of size on the bending strength of laminated veneer lumber. *Wood Science and Technology, 31(6), 3*99-413.